Available online at www.sciencedirect.com
SCIENCE DIRECT®
ELSEVIER
Global and Planetary Change 50 (2006) 63 – 82
GLOBAL AND PLANETARY CHANGE
www.elsevier.com/locate/gloplacha

Effective sea-level rise and deltas: Causes of change and human dimension implications

Jason P. Ericson [a,*], Charles J. Vörösmarty [a,b,1], S. Lawrence Dingman [b,2], Larry G. Ward [b], Michel Meybeck [c,3]

[a] *Water Systems Analysis Group, Institute for the Study of Earth, Oceans, and Space, University of New Hampshire, Durham, New Hampshire 03824, USA*
[b] *Earth Sciences Department, University of New Hampshire, Durham, New Hampshire 03824, USA*
[c] *UMR Sisphe, Universite de Paris VI, France Case 123, Tour 26, 4 Place Jussieu, 75257, Paris Cedex 05, France*

Received 19 January 2005; accepted 25 July 2005
Available online 24 January 2006

Abstract

An assessment is made of contemporary effective sea-level rise (ESLR) for a sample of 40 deltas distributed worldwide. For any delta, ESLR is a net rate, defined by the combination of eustatic sea-level rise, the natural gross rate of fluvial sediment deposition and subsidence, and accelerated subsidence due to groundwater and hydrocarbon extraction. ESLR is estimated under present conditions using a digital data set of delta boundaries and a simple model of delta dynamics. The deltas in this study represent all major climate zones, levels of population density, and degrees of economic development. Collectively, the sampled deltas serve as the endpoint for river basins draining 30% of the Earth's landmass, and 42% of global terrestrial runoff. Nearly 300 million people inhabit these deltas. For the contemporary baseline, ESLR estimates range from 0.5 to 12.5 mm yr^{-1}. Decreased accretion of fluvial sediment resulting from upstream siltation of artificial impoundments and consumptive losses of runoff from irrigation are the primary determinants of ESLR in nearly 70% of the deltas. Approximately 20% of the deltas show accelerated subsidence, while only 12% show eustatic sea-level rise as the predominant effect. Extrapolating contemporary rates of ESLR through 2050 reveals that 8.7 million people and 28,000 km^2 of deltaic area in the sample set of deltas could suffer from enhanced inundation and increased coastal erosion. The population and area inundated rise significantly when considering increased flood risk due to storm surge. This study finds that direct anthropogenic effects determine ESLR in the majority of deltas studied, with a relatively less important role for eustatic sea-level rise. Serious challenges to human occupancy of deltaic regions worldwide are thus conveyed by factors which to date have been studied less comprehensively than the climate change–sea-level rise question.

Keywords: deltas; reservoirs; sea-level rise; subsidence

* Corresponding author. Virginia Department of Conservation and Recreation, 101 N. 14th Street, 11th Floor, Richmond, Virginia 23219, USA. Tel.: +1 804 225 3389; fax: +1 804 371 0771.

E-mail addresses: Jason.ericson@dcr.virginia.gov (J.P. Ericson), charles.vorosmarty@unh.edu (C.J. Vörösmarty), ldingman@cisunix.unh.edu (S.L. Dingman), lgward@cisunix.unh.edu (L.G. Ward), meybeck@biogeodis.jussieu.fr (M. Meybeck).

[1] Fax: +1 603 862 0587.
[2] Fax: +1 603 862 2649.
[3] Fax: +33 133 1 4427 5125.

0921-8181/$ - see front matter © 2005 Elsevier B.V. All rights reserved.
doi:10.1016/j.gloplacha.2005.07.004

1. Introduction

Deltas are naturally dynamic coastal systems that are unique in their close links to both land-based fluvial and coastal ocean processes. They hold ecological and economic value throughout the world and are major centers of population and agriculture (Pont et al., 2002). In the presence of adequate fluvial sediment supply and minimal human influence, deltas generally maintain their integrity and/or continue to extend seaward (Sanchez-Arcilla et al., 1998). In fact, increased sediment load associated with the rise of agriculture and land clearing in upland drainage basins has accelerated the growth of many deltas over the past 2000 yrs (McManus, 2002). More recently, pandemic construction of reservoirs and diversions of freshwater for consumptive uses (Dynesius and Nilsson, 1994; Nilsson et al., 2005) have generally served to decrease the net sediment load of rivers (Walling and Fang, 2003; Vörösmarty et al., 2003; Syvitski et al., 2005). This decrease, along with isostatic loading factors, sediment compaction and accelerated subsidence of deltaic sediments resulting largely from local groundwater withdrawal and hydrocarbon extraction, has moved many deltas from a condition of active growth to a destructive phase (Milliman et al., 1989; McManus, 2002; Poulos and Collins, 2002; Day et al., 1995). The hazard is compounded by the global historical trend in eustatic sea-level rise and predictions of increasing rates of sea-level rise over the next century (Church and Gregory, 2001).

The interaction of these threats, their unique geography in different parts of the world, and the geomorphological distinctiveness of deltas makes a comprehensive global assessment of contemporary state and future sources of vulnerability in deltas difficult to establish. The stability of deltas is not defined by eustatic sea-level rise alone. The apparent rates of contemporary sea-level rise for individual deltas have been estimated, although measurement and their estimation remains problematic (Milliman et al., 1989). Studies have also estimated future scenarios based on anticipated conditions of fluvial input, delta subsidence, and acceleration of eustatic sea-level rise. Milliman et al. (1989) used estimates of eustatic sea-level rise, natural subsidence, and accelerated subsidence to estimate land loss under three future scenarios in the Nile and Bengal deltas. They estimated that under a worst-case scenario, habitable land loss in Egypt and Bangladesh between 1989 and 2100 could be 24% and 36%, respectively. A similar approach was used to evaluate the vulnerability of the Ebro delta (Sanchez-Arcilla et al., 1998).

This study expands and updates previous approaches, which have primarily considered individual deltas or a regional sample of deltas (Poulos and Collins, 2002). Our primary goal is to identify the principal factors determining the rate of ESLR across a sample of 40 deltas distributed throughout the world. Our approach considers both the fluvial and coastal contributions to this change. Explicit estimates of the impact of reservoirs and decreased discharge on sediment delivery to deltas are included in this assessment. We apply a GIS-based approach employing high resolution data sets to estimate contemporary rates of sea-level rise and lowland areas and populations at risk for 40 deltas (Fig. 1). This study also

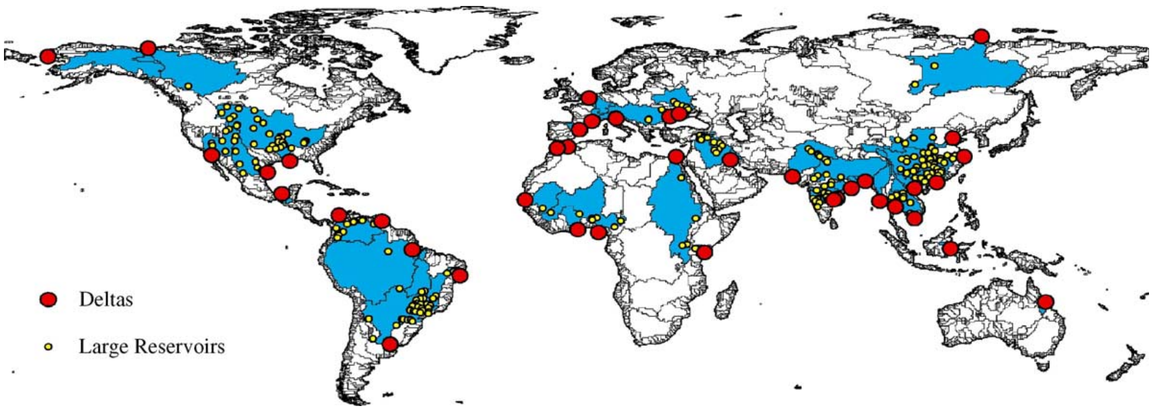

Fig. 1. Global distribution of the 40 deltas analyzed in this study, the potentially contributing drainage basin area of each delta (blue) and the large reservoirs (>0.5 km^3 maximum capacity) in each basin.

evaluates the implications of these trends over the next half-century.

2. Major forces shaping modern deltas

Effective sea-level rise (ESLR) is defined as the rate of apparent sea-level change relative to the delta surface. For an individual delta, ESLR is defined by the combination of eustatic sea-level rise, the natural rates of fluvial sediment deposition and subsidence, and any accelerated subsidence due to groundwater and hydrocarbon extraction, which is not compensated by deposition of fluvial sediment. The term effective sea-level rise used here is comparable to the concept of accretionary deficit (Stevenson et al., 1986). Relative sea-level rise (RSLR) (Day et al., 1995) is traditionally defined as the combination of eustatic sea-level change and subsidence, irrespective of the potential for sediment deposition, and is therefore a component within our definition of ESLR.

Common to all natural deltas is the ability of the associated fluvial system to deliver and deposit sediment more rapidly than local sea-level rise, subsidence or the rate sediment can be removed by coastal erosive processes (Wells and Coleman, 1984). The formation of most modern deltas began in the lower Holocene epoch (Stanley and Warne, 1994). Between 8000 and 6500 BP, global eustatic sea-level rise slowed following large meltwater additions associated with the transition from the last glacial maximum (Stanley and Warne, 1994). As the rate of eustatic sea-level rise declined, inputs of fluvial sediment began to accumulate along many coasts creating deltas throughout the world. Although Holocene delta formation has often been attributed to a number of factors including tectonic displacement, isostasy related to the loss of continental ice sheets, climate, drainage-basin morphology, and tectonics (Inman and Nordstrom, 1971), the dramatic deceleration of sea-level rise appears to be the dominant factor (Stanley and Warne, 1994). The long-term interaction between sea-level rise and fluvial input is suggestive of the sensitivity of modern deltas to changes in these two influences. However, today two fundamental factors are at play driving anthropogenic change in deltas: eustatic sea-level rise due to greenhouse warming and anthropogenic diversion of fluvial sediment destined for the coastal zone (Day et al., 1995).

2.1. Eustatic sea-level rise

Eustatic sea-level rose slowly during the last 3000 yrs until rates apparently began to increase during the middle of the nineteenth century (Church and Gregory, 2001). In the context of this study, eustatic sea-level rise refers to changes in mass of the oceans (i.e. addition of glacial meltwater) along with steric effects on the world's oceans (i.e. thermal expansion and salinity changes). Estimates of eustatic sea-level rise during the twentieth century typically range between 1.5 and 2 mm yr^{-1} (Miller and Douglas, 2004). With more than 100 million people living within 1 m of sea level (Douglas and Peltier, 2002), a sea-level rise of this magnitude presents significant threats to a large population over the span of decades. Although debate continues, it is widely believed that eustatic sea-level rise could accelerate during the twenty-first century resulting primarily from warming of the global climate and associated thermal expansion of the oceans, and the melting of the Greenland and Antarctic ice caps and glaciers (Church and Gregory, 2001).

2.2. Sediment delivery

Since the late 19th century, significant changes have taken place in the timing and quantity of sediment delivered to the world's coastal zone. A range of human activities has increased the sediment load in rivers, while others have decreased the load (Meybeck and Vörösmarty, 2005). For example, crop farming, deforestation, mining, and urbanization have led to higher sediment yields in some rivers. Conversely, improvements in erosion control practices have muted the increase during the second half of the twentieth century (GESAMP, 1994). A recent study of the annual sediment-load record of 145 major rivers indicates that approximately 50% of the rivers show a statistically significant upward or downward trend in sediment load over the period of record (Walling and Fang, 2003). Of these, the majority has undergone a significant downward trend. The overall pattern is thus one of reduced or little change in sediment reaching the coastal zone, despite widespread land cover change and increased local erosion.

Reservoir construction increased rapidly during the second half of the last century, with the number of registered dams growing 688% between the years of 1950 and 1986 (Vörösmarty et al., 1997). Although reservoirs serve a number of beneficial purposes, they also dampen peak flows and fragment river channels, which together with reservoir siltation reduce sediment delivery downstream of dams. Walling and Fang (2003) suggest that reservoir construction is the most important factor influencing contemporary land-ocean sediment fluxes. It has been estimated that 25–30% of the total global suspended sediment flux is intercepted by the population of approximately 45,000 reservoirs (with dams >15 m high) (Vörösmarty et al., 2003; Syvitski et al., 2005).

Other substantial impacts on sediment delivery to deltas include water diversions and consumptive losses, instream sediment mining, canal construction, and levee construction (Day et al., 1995). Competition for declining water supplies in heavily populated or irrigated basins reduces the conveyance capacity of rivers to transport sediment. Such has been the case in the Yellow River where discharge in the 1990s was only 1/3 of that for the 1970s, resulting in a sharp increase in the number of days of no-flow conditions in the river's lower reaches (Yang et al., 1998). Similarly, sediment discharge from the Yellow River to the Bohai Sea was 88% less in the 1990s than in the 1950s (Yang et al., 2002). The construction of human-made waterways for irrigation and transportation has trapped an already depleted sediment supply to the Nile delta. This entrapment of sediment is a key contributor to coastal erosion and land loss occurring on the Nile delta (Stanley, 1996). The instream mining of sand and gravel for construction aggregate has decreased the bed load of some rivers in areas of industrial growth (Sestini, 1996). The mining of fluvial sediment along with the trapping of sediment within the basin's reservoirs has resulted in uncompensated subsidence and local erosion in the Po delta (Cencini, 1998). Levees constructed along much of the length of the Mississippi River have confined the fluvial sediment to the river channel resulting in the delivery of the bulk of available sediment offshore rather than deposited in the delta. This decrease in sediment delivery is a significant factor contributing to land loss in the Mississippi delta (Kesel, 1988; Day et al., 2000).

2.3. Accelerated subsidence

Subsidence of unconsolidated deltaic sediments is a natural process occurring constantly in deltas. Subsidence occurs largely as a result of sediment compaction resulting from loading and dewatering of sediment. Also, the majority of deltas overlie large sedimentary basins that are gradually subsiding. Natural subsidence rates in deltas generally range from less than 1 mm yr^{-1} to more than 10 mm yr^{-1} (Jelgersma, 1996; Stanley and Warne, 1998). However, accurate measurements of subsidence within deltas are rare.

Subsidence in many deltas is accelerated by direct human action. As groundwater and petroleum are extracted from aquifer materials located within deltas, pore water pressures in aquifer and adjacent clay materials is decreased and the sediment compacts (Waltham, 2002). This compaction occurs in conjunction with natural subsidence and will be referred to here as accelerated subsidence. Accelerated subsidence has been documented in many deltas around the world and can locally reach rates upward of 300 mm yr^{-1} (Haq, 1997). Although rates this high are rare and subsidence tends to be uneven within a delta, accelerated subsidence in combination with natural subsidence can often be significantly greater than the rate of eustatic sea-level rise (Pont et al., 2002). In many deltas, particularly in Asia, populations have increased dramatically as people converge in urban coastal areas (Milliman, 1997). Deltas such as the Chao Phraya, Bengal, Yangtze and Nile have drawn large populations while maintaining substantial agricultural production. This has forced the increasing use of groundwater to supplement diminished surface-water supplies resulting in accelerated subsidence (Waltham, 2002). In addition, some deltas are the site of significant oil and gas accumulations and extraction as in the Niger, Magdalena, Mahakam, MacKenzie, and Mississippi deltas (Rainwater, 1975; Onu, 2003).

In addition to deltaic subsidence, some regions are affected locally by glacial isostatic adjustment (GIA). GIA is the gradual response of the earth's crust to the unloading of ice after the last glacial maximum (Douglas, 2001). The east coast of northern North America and the Fennoscandinavia region are still emerging today as a result of this unloading (Douglas and Peltier, 2002). The majority of deltas in this study are located at low and midlatitudes and are not subject to significant impact from GIA (Haq, 1997). The Mackenzie delta, however, is located in a region experiencing GIA-related emergence of approximately 1 mm yr^{-1} (Douglas and Peltier, 2002), and is accounted for in the methodology of this study.

2.4. Conjunctive effects

All of the anthropogenic factors mentioned above increase the rate of ESLR within deltas (Sanchez-Arcilla et al., 1998). As ESLR increases, deltaic lowlands become more vulnerable to inundation, flood events and erosion (Day et al., 1995). Rates of sandy shoreline erosion have been estimated to be approximately 100 times the rate of RSLR (Leatherman et

Table 1
Documented changes in deltas resulting from anthropogenic activities

Delta	Anthropogenic activities and induced change	References
Bengal	The densely populated Bengal Delta has seen increased subsidence rates resulting partially from the extraction of groundwater in both shallow and deep wells. RSLR rates in the Bengal Delta have been documented as high as 25 mm yr^{-1}. The ESLR in this delta threatens to worsen the damage of storm surges related to monsoonal storms.	Alam, 1996; Haq, 1997
Ebro	Decreased sediment loads resulting from sediment trapping behind the more than 170 dams in the Ebro drainage basin along with a strong longshore current have resulted in localized erosion and a general transformation from a prograding condition to a destructive phase of the delta.	Sanchez-Arcilla et al., 1998; McManus, 2002
Mississippi	The elimination of a major portion of fluvial sediment input to the delta from upstream reservoir construction and flood control levees has lead to a RSLR of 10 mm yr^{-1}. Estimated rates of wetland loss resulting from ESLR are as high as 100 km^2/yr in the delta.	Day et al., 2000; Wells, 1996
Moulouya	The Mohammed V reservoir in the Moulouya River basin has trapped approximately 94% of sediment supply to the coast of the largest river in Morocco. This reduction in sediment delivery along with impacts of recurrent droughts has resulted in significant coastal erosion and a gradual change from deltaic to estuarine conditions.	Snoussi and Haida, 2002
Niger	The Niger delta has seen both increased rates of coastal erosion (tens of meters per year) and significant subsidence in recent decades. Much of the coastal erosion is attributed to the trapping of sediment in reservoirs in the Niger drainage basin as well as a sharp decrease in sediment moving across the West African coast resulting from dam construction on the Volta River. Subsidence in the delta is attributed to the extraction of oil, which provides greater that 90% of Nigeria's export income.	Ibe, 1996; Collins and Evans, 1986
Nile	Since the closure of the Aswan High Dam in 1964 nearly all of the sediment carried above the dam has been trapped in the reservoir. This sediment trapping has resulted in a sharp decrease in sediment delivery to the delta. Coastal erosion, wetland loss and saltwater intrusion into delta aquifers have all been attributed to the decreased sediment input and associated subsidence. Coastal erosion rates close to the Rosetta and Damietta promontories range from 10 m yr^{-1} to greater than 100 m yr^{-1}. In addition to damming, a dense network of irrigation and drainage canals in the delta has trapped much of the remaining sediment preventing it from reaching the coastline.	Stanley and Warne, 1998; Fanos, 1995; Stanley, 1996
Po	From the 1950's until the 1970's, industrial dredging removed as much as 600×10^6 tons of sand from the riverbed. The mining of sediment along with the trapping of sediment in reservoirs in the basin, and accelerated subsidence associated with groundwater withdrawal have resulted in localized coastal retreat of hundreds of meters.	Cencini, 1998; Sestini, 1996
Rio Grande	The loss of sediment accretion due to dams, canals and levees along with continued subsidence has transformed the delta into an eroding feature and induced accelerated saltwater intrusion.	Stanley and Randazzo, 2001
Yellow	The sediment load of the Yellow has decreased significantly since the 1960's resulting from decreased water discharge and sediment trapping in reservoirs. Increased water consumption has resulted in the Yellow becoming a largely seasonal river. The rate of delta extension has slowed as the sediment load to the delta has decreased.	Jiongxin, 2003; Yang et al., 2002

al., 2000). Although ESLR can be partially compensated for by changes in river regulation and construction of levees, dikes, and seawalls, these measures are often expensive and usually offer temporary solutions to a growing problem. A survey of the literature indicates that such classes of anthropogenic factors

Table 2
Key attributes of the 40 deltas and references for delta extents where previously defined. Population data is from ORNL (2002), upstream basin area is from Vörösmarty et al. (2000) and the delta area extents were defined in this study

Delta	Continent	Delta area (1000 km^2)	Delta pop (millions)	Delta pop/km^2	Upstream basin area (1000 km^2)	Reference for delta extents
Amazon	South America	106	2.930	28	6720	–
Bengal	Asia	87.3	111.0	1,280	1730	Alam, 1996
Burdekin	Oceania	0.861	0.0058	7	121.0	–
Chao Phraya	Asia	20.8	13.70	659	175.0	–
Colorado	North America	6.34	0.3360	53	807.0	–
Danube	Europe	4.01	0.1560	39	788.0	Panin and Jipa, 2002; Giosan et al., 1999
Dniepr	Asia	0.354	0.0291	82	509.0	–
Ebro	Europe	0.338	0.0237	70	82.80	Maldonado, 1975; Wright et al., 1974
Godavari	Asia	3.43	1.830	534	315.0	Ramkumar, 2003; Bobba, 2002
Grijalva	Asia	10.4	1.040	100	118.0	–
Hong (Red)	Asia	4.59	5.710	1240	191.0	Pruszak et al., 2002
Indus	Asia	6.78	0.3910	58	1140	Wells and Coleman, 1984
Irrawaddy	Asia	30.4	9.720	319	421.0	Rodolfo, 1975; Wright et al., 1974
Krishna	Asia	2.00	0.5800	290	258.0	Rao and Sadakata, 1993
Lena	Asia	21.0	0.000079	0	2420	Rachold and Grigoriev, 2000
Mackenzie	North America	13.6	0.000001	0	1800	Carson et al., 1999
Magdalena	South America	3.89	1.880	484	261.0	–
Mahakam	Oceania	4.81	0.7060	147	71.10	Gastaldo et al., 1995
Mahanadi	Asia	5.91	3.880	656	141.0	Mohanti, 1993
Mekong	Asia	49.1	20.200	413	807.0	Kolb and Dornbusch, 1975
Mississippi	North America	28.8	1.790	62	3220	Kolb and Dornbusch, 1975
Moulouya	Africa	0.285	0.0777	273	59.30	–
Niger	Africa	17.7	3.730	211	2250	Ibe, 1996; Wright et al., 1974
Nile	Africa	24.9	47.800	1920	3870	Stanley and Warne, 1998
Orinoco	South America	25.6	0.0992	4	1070	–
Parana	South America	12.9	0.4440	35	2660	–
Po	Europe	0.729	0.0518	71	102.0	Cencini, 1998; Sestini, 1996
Rhine	Europe	3.81	1.940	509	230.0	–
Rhone	Europe	1.22	0.0921	76	99.00	Arnaud-Fassetta, 2003
Rio Grande	North America	13.9	2.030	145	805.0	Stanley and Randazzo, 2001
Sao Francisco	South America	0.757	0.0506	67	615.0	Coleman, 1976
Sebou	Africa	0.067	0.1130	1690	38.40	–
Senegal	Africa	3.24	0.2600	80	847.0	Barusseau et al., 1998
Shatt el Arab	Asia	3.85	0.4190	109	1030	–
Tana	Africa	0.481	0.00426	9	98.90	–

Table 2 (*continued*)

Delta	Continent	Delta area (1000 km^2)	Delta pop (millions)	Delta pop/km^2	Upstream basin area (1000 km^2)	Reference for delta extents
Volta	Europe	2.43	0.3850	158	398.0	Ly, 1980
Yangtze	Asia	34.1	42.10	1240	1800	–
Yellow	Asia	5.71	0.614	107	896.0	Yu, 2002; Jiongxin, 2003
Yukon	North America	5.02	0.00104	0	852.0	–
Zhujiang	Asia	9.08	11.700	1290	649.0	–

and their related ESLR impacts are pandemic in extent (Table 1).

3. Global sample of deltas

3.1. Methodology

Our methodology necessitates the definition of the geographic attributes of each delta. While previous studies identified the boundaries of many of the sampled deltas, a digital data set was not available. We created a digital data set of delta boundaries mapped at 30 arc sec or approximately 1 km (latitude × longitude) grid resolution (Fig. 1). Where available, the deltas were digitized based on the corresponding limits defined by aerial photographs, satellite imagery, maps and illustrations in previous studies ($n=23$) (Table 2). The remaining delta boundaries ($n=17$) were defined by

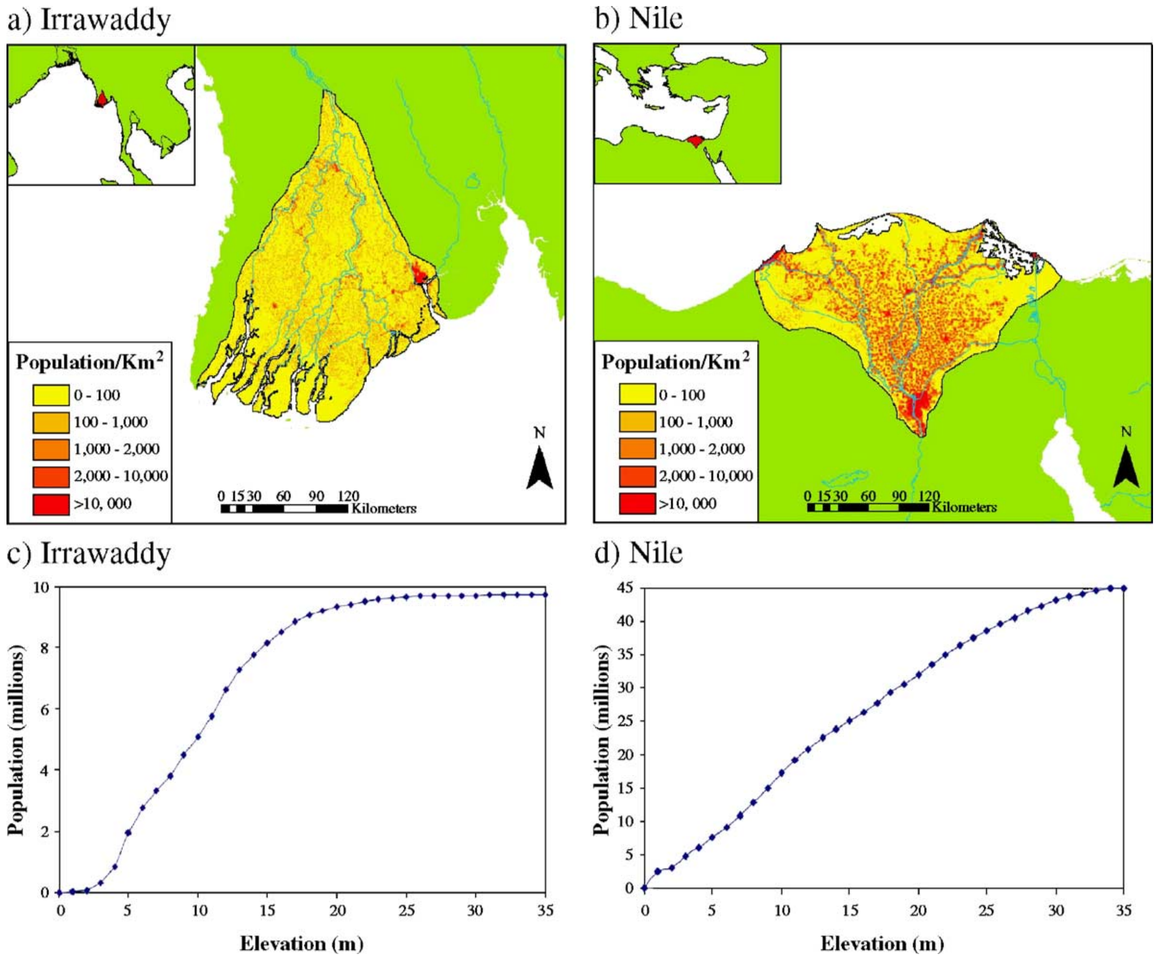

Fig. 2. (a,b) Delta extents defined for the Irrawaddy and Nile deltas and (c,d) the population distribution versus elevation for each. A dataset of delta extents for the 40 deltas was created for this study. The maps include the distribution of delta population mapped at 30 arc sec (latitude × longitude) resolution.

Table 3
Aggregate contribution of the 40 deltas used in this study with respect to fluvial and geographic attributes and compared with global totals

	40 deltas	Global land mass	% of global total	Mean for 40 deltas	Range
Area (million km^2)	0.580	133	0.43	0.014	6.7×10^{-5}–0.11
Area of upstream basins (million km^2)	41	133	30	1.02	0.0384–6.72
Delta population (millions 2002) [a]	288	6310	4.6	7.05	1×10^{-6}–111
Discharge to coastal zone (km^3 yr^{-1}) [b]	17,000	40,000	42	410	0.3–7300
Pre-disturbance sediment flux into coastal zone ($T*10^9$ yr^{-1}) [b]	6.8	20	34	171	0.0019–1.2
# of large reservoirs in basin (>0.5 km^3) [c]	264	714	37	7	1–40
Reservoir capacity in basin (km^3) [c]	2109	5170	41	88	0.55–587
Nitrogen flux from upstream (TG yr^{-1}) [d]	16.36	40.07	41	–	2.49×10^{-4}–3.82

[a] From Landscan data (ORNL, 2002).
[b] From Meybeck and Ragu (1996).
[c] From ICOLD (1998).
[d] From Green et al. (2004).

the presence of deltaic soils, topography, and the position and upstream limit of distributary channels (FAO, 1974; USGS, 2003).

If not previously identified, we defined delta boundary as the subaerial coastal lowlands where predominant soils are alluvial in origin. The upstream limit of distributaries is used as an indicator of the upstream boundary of the delta. Where the soil and distributary data were insufficient, topographic data was used to infer delta boundaries (USGS, 2003). Population data for each delta were taken from the 30 arc sec (latitude × longitude) resolution Landscan data set (ORNL, 2002). The population and elevation within each grid cell were sampled and cumulative distribution functions of population versus elevation were created for each delta (USGS, 2003) (Fig. 2). The population data were also used to determine population density distributions within each delta. The digitized deltas were also linked to a digital global river network at 30-min (latitude × longitude) spatial resolution (STN-30) to identify the contributing drainage basin area and discharges for each delta (Vörösmarty et al., 2000; Fekete et al., 2001).

3.2. Representative nature of sample delta systems

To identify the primary agents of change in modern deltas, we selected a sample of 40 deltas for study (Fig. 1), with the majority included in previous compendiums of the world's large deltas or showing particularly sensitivity to change (Coleman and Wright, 1971; Wright et al., 1974). A concerted effort was made to select deltas reflecting a diverse range of climatic zones, coastal settings, level of economic development, and population densities.

The sample of deltas presented in this study constitutes a reasonable representation of the global population of deltas. All five Koeppen climate classes are represented by the deltas. The representative nature of the 40 deltas in this study is illustrated by the comparison of the cumulative contribution of the 40 deltas to a range of geographic and fluvial characteristics against the global estimates of these characteristics (Table 3). Although the deltaic area represented by our deltas is only 0.4% of the total non-glacierized land surface area of the globe, the human population of these deltas comprises approximately 4.6% of the global population. Additionally, the average population density of our deltas is approximately an order of magnitude greater than the average population density of the globe. The population found in Asian deltas is far greater than the deltaic populations of the other continents; however, Africa has the highest population density among all regions (Table 4). The majority of deltas are more densely populated than their upstream contributing area

Table 4
Population and population density data for the 40 deltas in this study

River	Delta area (1000 km^2)	Delta pop 2002 [a] (millions)	Delta pop/ km^2 2002 [a]	Est. delta pop 2050 [b] (millions)	Est. delta pop/km^2 2050 [b]
Africa	49.10	52.30	1070	94.60	1930
Asia	284.0	222.0	782	329.0	1160
Europe	10.10	2.260	224	2.440	242
North America	78.10	5.190	66	7.540	97
South America	149.0	5.410	36	7.400	50
Oceania	5.670	0.712	126	12.10	2130
World	576.0	288.0	500	453.0	934

[a] From Landscan data (ORNL, 2002).
[b] Delta population in 2050 estimated using country level population growth estimates for 2003–2050 from the Population Reference Bureau (PRB, 2004).

(Fig. 3a). A number of large, economically vital cities are located in the sample of deltas including Shanghai, Bangkok, Cairo, Cartagena and New Orleans. The large populations and high population densities in these deltas, particularly in rapidly developing deltas in Southeast Asia, make the evaluation of current and future risk of ESLR essential.

Similarly, the rivers feeding the deltas we assess contribute a large part of the global flux of fluvial sediment, water and nutrients to the coastal zone (Table 3). The contributing drainage basin area of the rivers feeding into the deltas analyzed represents about 30% of the non-glacierized land surface area of the globe. The percentages of the global fluvial water and sediment discharge to the coastal zone moving through the deltas in our study are 42% and 34%, respectively (Meybeck and Ragu, 1996). Nitrogen flux from upstream into our sample of deltas makes up 41% of the global total estimated nitrogen flux to the coastal zone (Green et al., 2004). Also, the river basins draining into these deltas contain 37% of the global population of large reservoirs, 41% of the global reservoir capacity and have a mean upstream sediment trapping efficiency of 47% (ICOLD, 1998; Vörösmarty et al., 2003) showing that these basins, cumulatively, have undergone marked alteration to their water and fluvial sediment discharge.

4. Estimation of effective sea-level rise

We estimate ESLR by examining the relationship between fluvial sediment input, the natural rate of delta subsidence, accelerated subsidence, and the contemporary rates of eustatic sea-level rise. The methodology used in this study relies on a number of assumptions related to the scale being examined. These assumptions include uniform eustatic sea-level rise and uniform subsidence within each delta. Although these

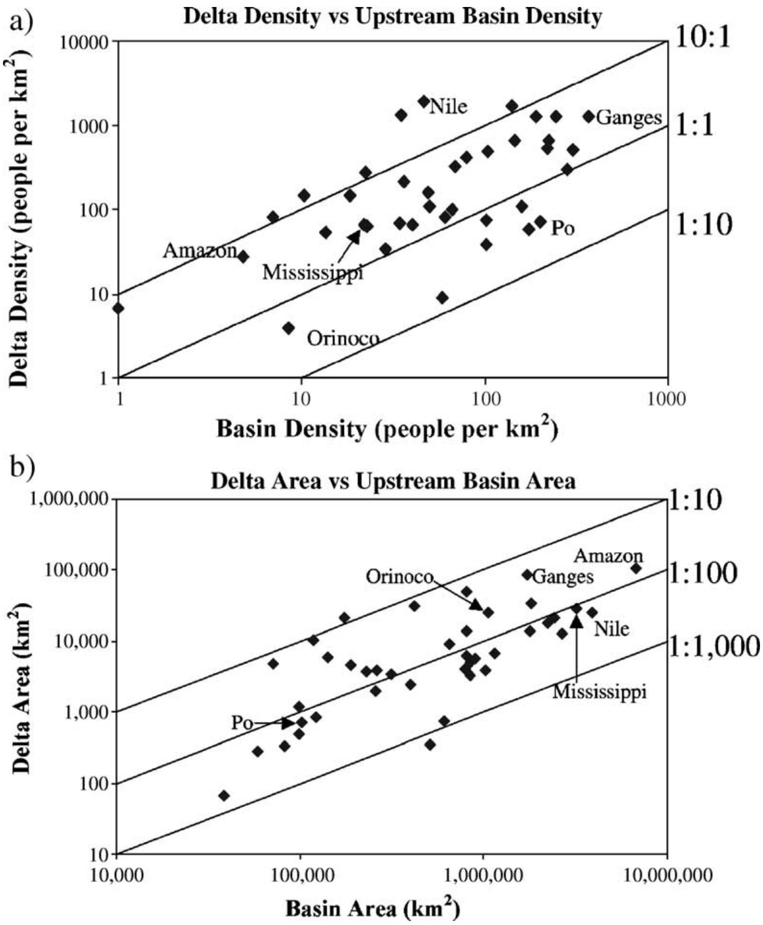

Fig. 3. (a) Comparison of the population density in the 40 sampled deltas against the average population density of the upstream drainage basin. (b) Plot of the delta area and the upstream contributing basin area.

assumptions are not universal in all cases, they do not detract from the overall results and conclusions of the study.

For the purposes of this study we define (i) "natural conditions" as a setting in which human impacts are considered minimal, (ii) a "contemporary baseline" as contemporary sea-level conditions taking into account accelerated eustatic sea-level rise, accelerated subsidence and sediment trapping in upstream reservoirs, and (iii) "future conditions" as contemporary baseline conditions extrapolated for each delta over the period 2000–2050. The purpose of depicting the natural conditions is to have a reference upon which to compare the contemporary baseline conditions in order to determine what sources of change are dominant in each delta.

This method assumes that under natural conditions, deltas are in equilibrium and that the effective sea-level rise (ESLR) on net is zero. Natural deltaic subsidence and eustatic sea-level rise are offset by the accretion of fluvial sediment and organic deposition (Fig. 4a) (Milliman et al., 1989; Sanchez-Arcilla et al., 1998; Reed, 2002). The net ESLR (N_{eslr}) under natural conditions is calculated as:

$$N_{\mathrm{eslr}} = G_{\mathrm{slr}} + G_{\mathrm{ns}} - G_{\mathrm{nfluv}} = 0 \tag{1}$$

where G_{slr} is the gross historic eustatic sea-level rise, G_{ns} is the gross natural deltaic subsidence, and G_{nfluv} is the gross natural accretion of fluvial sediment and organics. In this case we assume that the relative sea-level rise ($\mathrm{RSLR} = G_{\mathrm{ns}} + G_{\mathrm{slr}}$) is equal to the gross accretion of fluvial sediment and organics (G_{nfluv}). A value of 1.5 mm for G_{slr} is applied globally and G_{ns} is taken from literature values. G_{nfluv} is then calculated based on the assumption that N_{eslr} equals zero. N_{eslr} is expressed from the reference frame of each delta, such that terms in Eq. (1) are positive whenever they contribute to an apparent increase in sea level relative to the delta.

Under the contemporary baseline influenced by anthropogenic forcings, changes to the fluvial sediment supply, groundwater and hydrocarbon extraction inside deltas, and any increase in the rate of eustatic sea-level rise combine in unique ways to determine net ESLR in

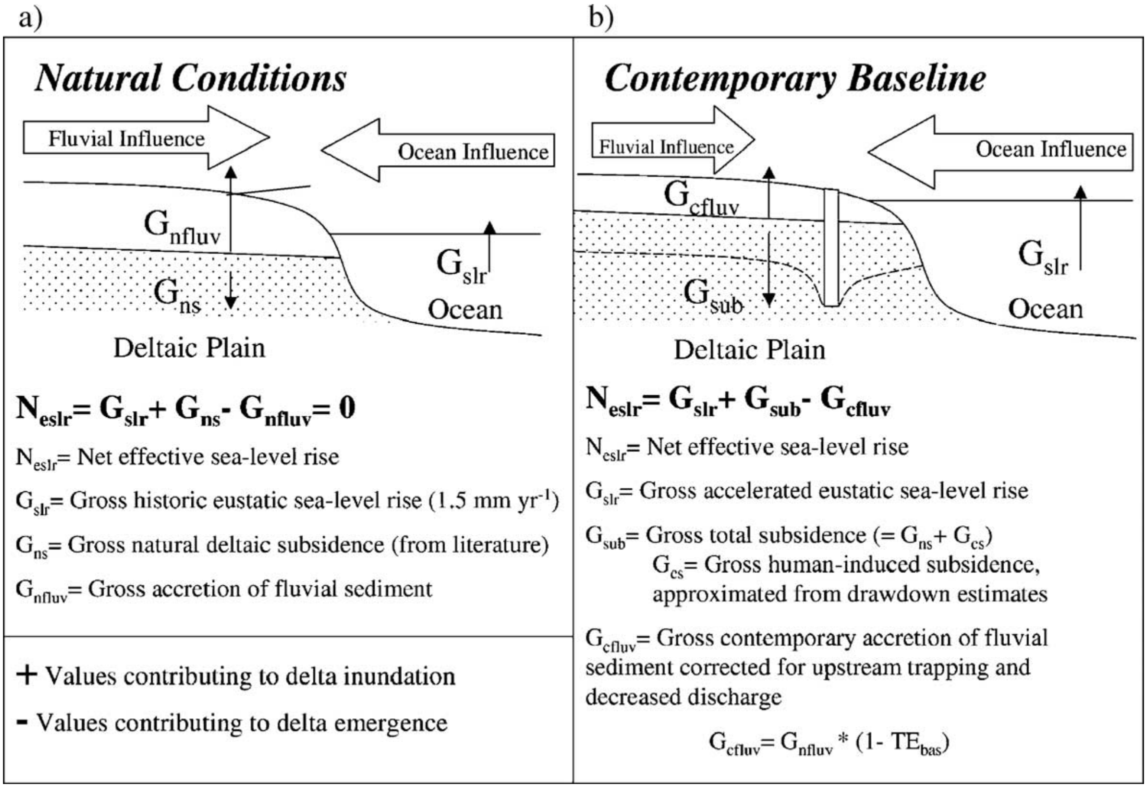

Fig. 4. Schematic of the calculation of effective sea-level rise (ESLR) for individual deltas under (a) natural and (b) contemporary conditions. Under natural conditions we assume that fluvial sediment accretion and organic deposition offset natural deltaic subsidence and eustatic sea-level rise, resulting in no net ESLR. The ESLR under contemporary conditions is a function of any increase in the rate of eustatic sea-level, changes to fluvial sediment supply and accelerated subsidence in the delta.

each delta (Fig. 4b). Net ESLR under anthropogenic conditions is thus equal to the sum of change in the rate of fluvial accretion, the increase in total deltaic subsidence, and the rate of eustatic sea-level rise. We define the net ESLR under anthropogenic conditions as:

$$N_{\text{eslr}} = G_{\text{slr}} + G_{\text{sub}} - G_{\text{cfluv}} \quad (2)$$

where G_{slr} is the contemporary rate of eustatic sea-level rise, G_{sub} is the total gross subsidence (natural plus human-accelerated subsidence) and G_{cfluv} is the gross contemporary fluvial sediment accretion reflecting change arising from upstream trapping in impoundments. The G_{cfluv} term is determined by the net basin trapping efficiency for river sediment from reservoir siltation and flow diversion. Our methodology assumes a uniform rate of subsidence and sediment accretion across the extent of each individual delta. Although subsidence can vary throughout an individual delta, the assumption that subsidence is uniform is suitable for the synoptic scope of this study. The method for estimating each component of Eqs. (1) and (2) is described below.

4.1. Fluvial sediment input

The gross accretion of fluvial sediment under natural conditions (G_{nfluv}) was computed as described above. The gross accretion of fluvial sediment after upstream trapping (G_{cfluv}) is calculated as the product of gross accretion of riverine sediment and organics under natural conditions (G_{nfluv}) and the proportion of sediment trapped upstream by reservoirs or entrained in flow diversions and consumptive losses. We apply the approach of Vörösmarty et al. (2003) to estimate the sediment trapping potential of reservoirs. The change in river-water residence time and trapping efficiency associated with large reservoirs (storage >0.5 km^3) (a function of the individual reservoir change in residence time) is determined. A basin-wide trapping efficiency due to reservoirs (TE_{bas0}) is then calculated as a discharge-weighted function of the trapping efficiency of the impounded portion of the basin.

The trapping efficiency estimate of the reservoirs is further modified to account for upstream water withdrawals. Where data of natural and contemporary water discharge are available (Meybeck and Ragu, 1996; Dynesius and Nilsson, 1994), a trapping efficiency (TE_{bas}) considering changes in water discharge is calculated as follows:

$$\text{TE}_{\text{bas}} = 1 + (Q_{\text{cont}}/Q_{\text{nat}}) * (\text{TE}_{\text{bas0}} - 1) \quad (3)$$

where Q_{cont} is the contemporary river water discharge and Q_{nat} is the natural river water discharge.

The contribution of small reservoirs (<0.5 km^3 capacity) to sediment trapping is estimated by extrapolations derived from the characteristics of large reservoirs (Vörösmarty et al., 2003), to determine the numbers and storage volumes involved and to spatially distribute them within the basins. The estimate of the contribution of small reservoirs to the overall trapping efficiency gives an approximation of the magnitude of small reservoir sediment trapping in each basin. Using these relationships, the TE_{bas} in each basin is adjusted for small reservoirs. The fluvial sediment after upstream trapping (G_{cfluv}) is then calculated as:

$$G_{\text{cfluv}} = G_{\text{nfluv}} * (1 - \text{TE}_{\text{bas}}). \quad (4)$$

Our method of estimating basin trapping efficiency does not take into account variations in the timing of sediment or water discharge within the basins, and thus reflects overall mean conditions. The method also does not take into account the loss of reservoir capacity corresponding to the filling of reservoirs with sediment.

4.2. Subsidence

Natural rates of subsidence (G_{ns}) are taken from published values where available and generally range from less than 1 to 10 mm yr^{-1} (Jelgersma, 1996). These values include both shallow subsidence and deeper underlying tectonic movements. We use published values of natural deltaic subsidence where available, and use an average value for deltas where published estimates are unavailable (2.5 mm yr^{-1}).

The estimation of accelerated subsidence is problematic due to spatial and temporal variations based on the location and intensity of the human activities causing the acceleration. Published values of accelerated subsidence vary widely and have been documented to reach rates of up to 300 mm yr^{-1} locally (Haq, 1997). Previous investigators have estimated accelerated subsidence over an entire delta resulting from groundwater and petroleum withdrawal as three times the natural rate of subsidence (Milliman et al., 1989; Milliman, 1997). In the absence of reliable data, this approximation provides a rough estimate of the possible rates of accelerated subsidence. We use the factor of three times the natural subsidence rate to define the upper limit of the potential accelerated subsidence based on the assumption that accelerated subsidence is a direct result of the magnitude of anthropogenic influence on delta sediments. We assume that a delta with a significant extraction of water and a correspondingly high draw-down of the water table will undergo significant accelerated subsidence. In the following explanation, we calculate water table draw-down values to adjust the intensity of accelerated subsidence. Draw-down resulting from groundwater withdrawals is calculated as:

$$\Delta h = V_{\mathrm{gw}}/(A_{\mathrm{s}} * S_{\mathrm{y}}) \quad (5)$$

where Δh is the draw-down, V_{gw} is the volume of groundwater withdrawn, A_{s} is the area of the delta region, and S_{y} is the specific yield of the aquifer. Although variable, a specific yield value of 0.2 is considered representative of deltaic sediments (Fetter, 2001). Calculation of draw-down for each delta is described below.

Observations of groundwater withdrawal for individual deltas are rare, so a method was developed to estimate water use. Total agricultural water-use data for each country for 1998 are taken from the AQUASTAT database (FAO, 2004). The water-use data include groundwater extractions as well as direct removal from surface water bodies. For countries where the percent of total irrigation water used that is groundwater is reported (86 out of 203), the volume of groundwater extraction is calculated as the product of this percent and the total agricultural water use. The percent of irrigation use as groundwater for countries without reported values is approximated as a function of the national maximum climatic moisture index value (CMI). The CMI is a simple index depicting the moisture conditions at a particular site (Wilmott and Feddema, 1992), with $\mathrm{CMI}=(P/\mathrm{PET})-1$ when $P<\mathrm{PET}$ and $\mathrm{CMI}=1-(\mathrm{PET}/P)$ when $P \geq \mathrm{PET}$. The CMI ranges from 1 to −1, with wet climates showing positive values, dry climates negative. A strong relationship ($r^2=0.77$) was found between the maximum CMI by country and the reported percent of irrigation as groundwater:

$$I_{\mathrm{gw}} = -33.6 * \ln(\mathrm{CMI}_{\max}) + 25.1 \quad (6)$$

where I_{gw} is the percent of irrigation withdrawals as groundwater and $\mathrm{CMI}_{\max}$ is the maximum CMI value for a particular country. In this case, the $\mathrm{CMI}_{\max}$ is the computed CMI+1, to ensure positive values and thus permit use of the logarithmic relationship. This relationship implies that humid climates are less reliant on groundwater resources than arid climates.

The calculated volume of groundwater withdrawn for agriculture for each country was then geospatially disaggregated by distributing it over irrigated areas (Siebert et al., 2002) according to irrigation need. Irrigation need is assumed to be the difference between the potential evapotranspiration (PET) and the actual evapotranspiration (AET). The Shuttleworth–Wallace method was used to calculate PET, and AET was computed using the UNH Water Balance Model (Vörösmarty et al., 1998; Federer et al., 2003) and a physically based PET function (Shuttleworth and Wallace, 1985). The groundwater withdrawals, disaggregated at 30-min (latitude × longitude) spatial resolution, are then used to calculate the water table draw-down in each delta. Calculated draw-down does not account for saltwater intrusion related to groundwater withdrawal. The draw-down values were compared with known maximum draw-down values in aquifers of India (~3 m yr^{-1}) (Bansil, 2004) and correspond well with groundwater conditions in the Mid-western and South-western United States.

The maximum draw-down found in each delta was used to approximate the rate of accelerated subsidence. The highest maximum draw-down value for all 40 deltas is assumed to result in an accelerated subsidence rate of three times the rate of natural subsidence (Milliman, 1997). The multiplier for the others deltas is calculated as the ratio of the individual draw-down in each delta to the maximum draw-down. For example, if the hypothetical maximum draw-down in the sample of deltas is 4 m yr^{-1} and the draw-down in Delta A is 2 m yr^{-1}, the accelerated subsidence for Delta A is approximated as 1.5 times ($3*2$ m yr^{-1}/4 m yr^{-1}) its natural subsidence rate. If an individual delta is identified as a location of significant petroleum or natural gas production, an additional 1 mm yr^{-1} of accelerated subsidence is added (Raghavendra Rao, 1991). Any land movement related to GIA is considered to be included in estimates of natural subsidence.

4.3. Eustatic sea-level rise

An estimate of contemporary eustatic sea-level rise of 2 mm yr^{-1} (Church and Gregory, 2001; Douglas, 2001; Douglas and Peltier, 2002; Miller and Douglas, 2004) (which includes both natural and recent anthropogenic influences) is applied, augmenting the rate of eustatic sea-level rise of 1.5 mm yr^{-1} used to define natural conditions (following the mid nineteenth century increase). These estimates are in keeping with IPCC estimates ranging from 1 to 2 mm yr^{-1}. The approximation of contemporary ESLR is applied to each delta based on the estimates of sediment trapping and flow diversions, natural subsidence, accelerated subsidence, and eustatic sea-level rise as described above. These estimates are then extrapolated into the twenty-first century to assess the land area and human population

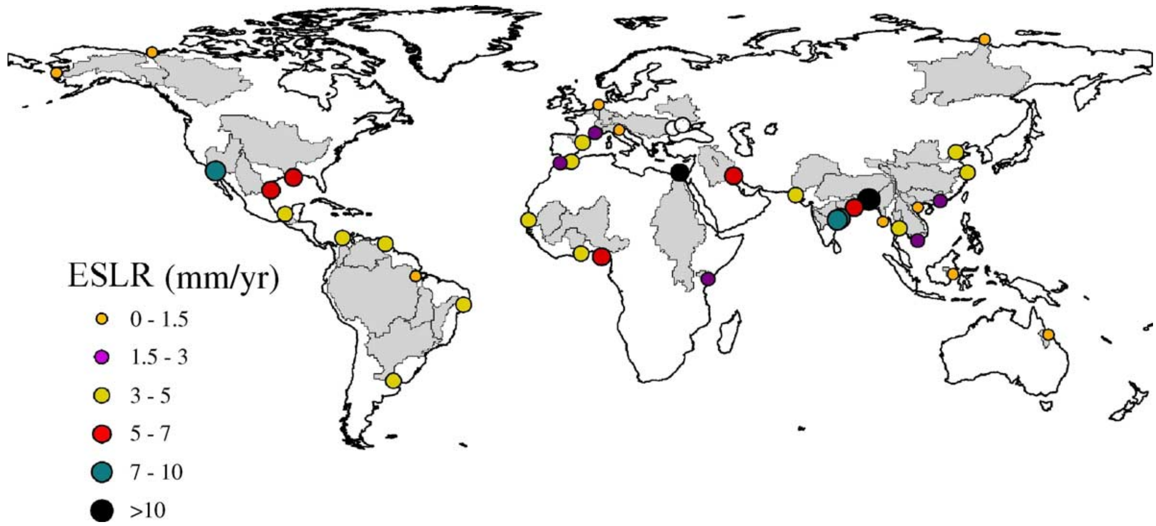

Fig. 5. Global distribution of ESLR under baseline conditions for each of the 40 deltas in this study. The upstream drainage basin for each delta is highlighted for presentation purposes. This figure represents contemporary conditions.

potentially at risk should current rates remain unchanged. Although it is widely believed that rates will accelerate during the twenty-first century, we only consider contemporary estimates of eustatic sea-level rise (Nicholls, 2002). Our results are therefore conservative. It should be mentioned that our results of ESLR assume the accuracy of these eustatic sea-level rise estimates. Although the IPCC rates represent the best available estimates, the certainty of these estimates should be considered when reviewing this study's conclusions.

5. Results

5.1. Contemporary baseline ESLR condition

Constructing a contemporary baseline for ELSR enables us to assess the current importance of each major factor contributing to deltaic sea-level rise. The global distribution of ESLR under the contemporary baseline condition (Fig. 5) shows estimates ranging from 0.5 to 12.5 mm yr^{-1} with a mean value of 3.9 mm yr^{-1} and a median of 4.0 mm yr^{-1}. The three highest ESLR estimates are for deltas in south Asia, which tend to be densely populated, agriculturally active and have strongly regulated drainage basins. Table 5a summarizes the characteristics of these ESLR estimates for each continent.

When aggregated to the continental scale, several patterns in the distribution of ESLR can be seen. For all continents except Oceania (with small sample size), mean ESLR varies between 2.6 and 4.6 mm yr^{-1}, mean trapping efficiencies between about 50% and 75% and accelerated subsidence between 0.1 to over 2 mm yr^{-1}. North American and Asian deltas have the highest average ESLR estimates of 4.5 and 4.6 mm yr^{-1}, respectively. The North American deltas have high basin trapping efficiency (75%) and a moderate rate of accelerated subsidence (1.4 mm yr^{-1}), illustrating the importance of the contributions of both sediment loss and accelerated subsidence to ESLR estimates. It is noted that the Mississippi delta has a high rate of subsidence that is an exception when compared with other North American deltas. A moderate mean basin trapping efficiency (53%) and the highest mean accelerated subsidence rate (2.1 mm yr) combine to produce high rates of ESLR for the Asian deltas. The remaining regions all show relatively low rates of accelerated subsidence (<0.5 mm yr^{-1}).

Table 5a
Regional distribution of ESLR estimates for deltas, upstream basin sediment trapping efficiency and accelerated subsidence under baseline conditions

	n	Mean ESLR (mm/yr)	Mean TE (%)	Mean accelerated subsidence (mm/yr)
Asia[a]	14	4.6	53.2	2.1
North America[b]	6	4.5	75.1	1.4
South America	5	3.5	66.4	0.3
Europe[c]	6	2.6	51.8	0.1
Africa	7	4.4	75.9	0.5
Oceania[d]	2	1.0	0.0	0.5
Total	40	3.9	57.9	1.1

[a] Asia is defined as including the Middle East and Turkey.
[b] North America includes Mexico and Central America.
[c] The eastern border of Europe is defined as Russia's western border.
[d] Oceania includes Australia, New Zealand, and Indonesia.

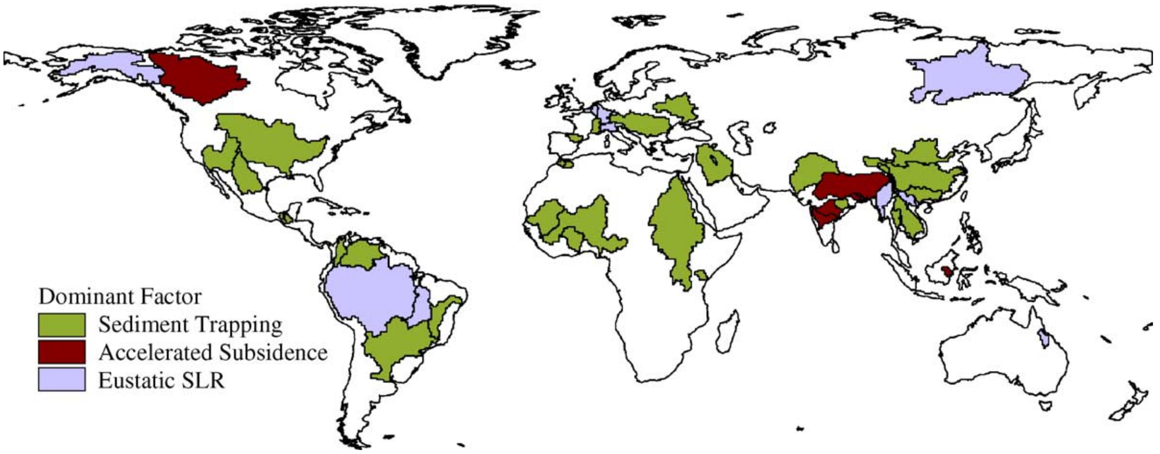

Fig. 6. Dominant factor in estimate of baseline ESLR for each of the 40 deltas. Sediment trapping is the dominant factor for 27 deltas, eustatic sea-level rise is the dominant factor for 8 deltas and accelerated subsidence is the dominant factor for 5 deltas. This represents the major forces at play under contemporary conditions.

5.2. Dominant sources of effective sea-level rise

We define the dominant factor in the contemporary baseline ESLR estimate for each delta as the deviation from natural conditions that results in the largest proportional contribution to the computed total contemporary baseline ESLR (Fig. 6). The loss of fluvial sediment resulting from trapping in reservoirs and flow diversion is the dominant factor in ESLR for a majority (27) of the sample deltas (Table 5b). This result is in agreement with recent studies that recognize the influence of reservoir construction on fluvial sediment flux to the coastal zone (Walling and Fang, 2003; Vörösmarty et al., 2003). This study identified the dominant ESLR factor for nine deltas that were also included in a recent study of long-term sediment records (Walling and Fang, 2003). Walling and Fang identified five of these rivers that showed a significant downward trend in suspended sediment load. The present study identified upstream sediment trapping as the dominant factor in ESLR for the deltas of all five of these rivers. Of the remaining four, sediment trapping is identified as the dominant factor in two cases and accelerated subsidence in two cases. Our results also support observations about the dominant factor in deltaic land loss in individual deltas including the Indus, Nile, Ebro, Volta and Niger deltas (Collins and Evans, 1986; Stanley and Warne, 1998; Sanchez-Arcilla et al., 1998; McManus, 2002).

A continental approach illustrates the dominance of sediment trapping for most regions. Sediment trapping is the dominant factor in ESLR for all seven of the African deltas studied, in part a function of the large mean size of African reservoirs and high trapping efficiency inside the upstream basins (Vörösmarty et al., 2003). Sediment trapping is also the dominant factor for a majority of deltas in North America, South America and Europe. Asia shows a more even distribution with the dominant factor being sediment trapping for eight of its deltas, accelerated subsidence for three deltas and accelerated eustatic sea-level rise for the remaining three. Because Asian deltas tend to be highly populated and demand for water resources is correspondingly high, accelerated subsidence resulting from groundwater extraction plays a larger role than in other regions. Although African deltas have an even higher population density, water use is generally less intensive (Vörösmarty et al., 2005). Sediment trapping is the predominant factor across all regions with the exception of Oceania. However, this study considers only two deltaic systems in Oceania and this result should not be considered representative of the region as a whole.

Table 5b
Regional distribution of the dominant factor in ESLR under baseline conditions for the 40 deltas in this study

	n	Dominant factor in ESLR		
		Sediment trapping	Accelerated subsidence	Eustatic sea-level rise
Asia	14	8	3	3
North America	6	4	1	1
South America	5	4	1	0
Europe	6	4	2	0
Africa	7	7	0	0
Oceania	2	0	1	1
Total	40	27	8	5

5.3. Validation of ESLR estimates

The contemporary baseline condition assumes that maximum accelerated subsidence from groundwater withdrawal is three times the natural rate. Although this assumption has been used in previous studies of ESLR (Milliman, 1997), this is largely untested. Our estimates of eustatic sea-level rise (G_{slr}) plus subsidence (G_{sub}) are compared against independent published measurements of contemporary RSLR for 9 of the sampled deltas (Fig. 7). The measurement of RSLR in deltas only accounts for eustatic sea-level rise (G_{slr}) and subsidence (G_{sub}) and not the accretion of sediment (G_{cfluv}) (Day et al., 1995). This allows for the comparison of our method of estimating accelerated subsidence (G_{cs}) with published measurements and an evaluation of its accuracy.

The independent estimates are for deltas in Asia, Europe and North America and are biased towards the more heavily populated or economically important deltas. Our estimates nonetheless agree well with many of the published values and demonstrate that this method of estimating accelerated subsidence is generally valid. However, for four of the deltas we underestimate the measured RSLR to varying degrees. These results imply that our model captures many of the factors contributing to accelerated subsidence for these deltas but does not account for all sources and should therefore be viewed as conservative.

The underestimates for several of the deltas have seemingly obvious explanations. In the Po delta, we underestimate the measured RSLR by 2.9 mm yr^{-1}. The discrepancy is likely a result of accelerated subsidence not accounted for in our estimate. A significant portion of the groundwater withdrawn in the delta is used for industrial purposes and is not accounted for in this study (Cencini, 1998). Additionally, extraction of methane-bearing groundwater from underlying sediments between 1938 and 1964 resulted in significant subsidence, which has continued through recent times (Cencini, 1998; Bondesan et al., 1986).

In the case of the Mississippi delta, our estimate of the contemporary RSLR is 7 mm yr^{-1} and the published measured RSLR value is 10 mm yr^{-1} (Kesel, 1989; Penland and Ramsey, 1990; Wells, 1996). Accelerated subsidence related to industrial withdrawals, not accounted for in our study, is likely responsible for the discrepancy (Wells, 1996).

For the Yangtze delta, the published estimate of RSLR is for the Shanghai region where much of the groundwater extraction is for domestic and industrial use (Ren and Milliman, 1996; Wang, 1998). The published measurement is not representative of the entire delta, and accelerated subsidence is presumably smaller in regions of lower domestic and industrial withdrawals. At the same time, our estimate does not include these withdrawals and would not detect the corresponding accelerated subsidence in urban regions of the deltas.

These examples illustrate that our model underestimates accelerated subsidence in cases where accelerated subsidence is in part related to industrial and domestic water withdrawals. There are no globally

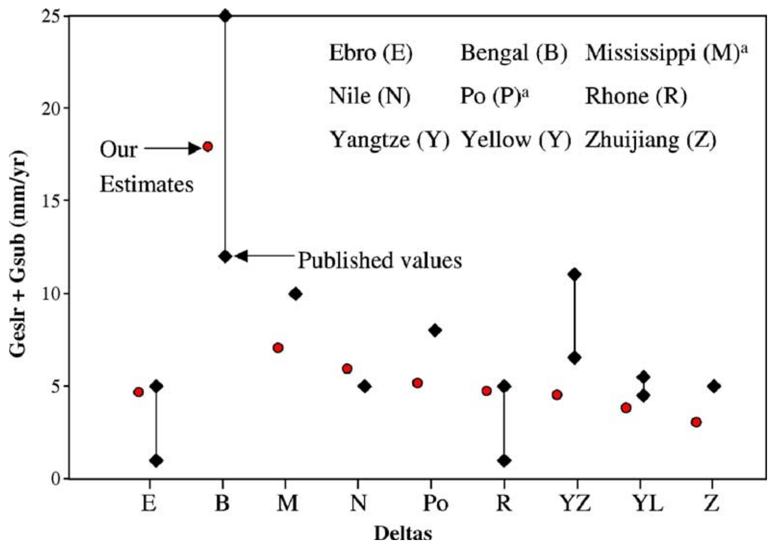

Fig. 7. Comparison of baseline estimates against published estimates for RSLR ($G_{sub}+G_{slr}$) for the Ebro (L'Homer, 1992), Bengal (Haq, 1997), Mississippi (Penland and Ramsey, 1990), Nile (Stanley, 1990), Po (Sestini, 1992), Rhone (L'Homer, 1992), Yangtze (Wang, 1998), Yellow (Wang, 1998), and Zhuijiang (Ren, 1993) deltas.

coherent estimates distinguishing between withdrawals of surface and groundwater, so the overall impact of domestic and industrial withdrawals on the sample of 40 deltas is difficult to establish. The effect is unlikely to significantly change our basic conclusion regarding the dominance of sediment trapping/flow diversion in ESLR for the majority of the deltas considered. However, these withdrawals play a significant role in ESLR for several of the deltas, particularly the Yangtze, Chao Phraya and Po deltas.

5.4. Baseline ESLR condition extended through 2050

The baseline contemporary ESLR estimates were extrapolated from 2000 through 2050 to estimate potential vulnerability to sea level incursion into deltas. The populations affected and land areas potentially inundated (Table 6) were determined from population-elevation and area-elevation distribution curves for individual deltas as given in Fig. 2c, d. Future populations were estimated from national population growth statistics through 2050 and applied spatially according the Landscan population data distributions (ORNL, 2002; PRB, 2004). It should be noted that these estimates do not consider human response to rising waters such as abandonment or protection of land with seawalls and embankments. Moreover, these estimates do not take into account coastal erosion from storm impacts.

The total population in our 40 deltas potentially affected by inundation under the contemporary baseline ESLR condition by year 2050 is approximately 9 million. Nearly 75% of the total population impacted is in the Asian deltas, reflecting both the bias towards these deltas in our study ($n=14$) and their high populations (Table 7). The Bengal delta has by far the largest potential impact (3.4 million affected), but this is only 1.8% of the estimated Bengal delta population in 2050. Similarly, the average percentage of the total delta population affected across Asian deltas is relatively low (2.0%) in comparison with percentages in some other regions. North American deltas show the highest percentage (6.8%) of its deltaic populations experiencing potential inundation and the highest percentage of delta area impacted (9.7%).

The ranges for the percentage of the total delta population at risk and percentage of total delta area impacted by continent are 1.5–6.9% and 2.5–9.7%, respectively (Table 7). The percentage of the global delta populations and delta land made vulnerable by ESLR in the sample of 40 deltas are 2.0 and 4.9%, respectively.

Table 6
Distribution of the total population potentially impacted, percentage of delta population influenced and the delta area impacted for each delta under baseline ESLR conditions extended from 2000 through 2050

Delta	Population at risk	% delta population at risk	% delta area potentially lost
Amazon	69,300	1.89	2.45
Bengal	3,430,000	1.78	5.50
Burdekin	24	0.28	1.33
Chao Phraya	12,300	0.01	0.34
Colorado	544	0.11	3.35
Danube	3150	2.56	4.18
Dnepr	1300	5.60	7.31
Ebro	470	2.00	2.19
Godavari	453,000	16.2	22.5
Grijalva	26,700	1.76	5.59
Hong (Red)	70,500	0.85	0.95
Indus	7200	0.79	2.73
Irrawaddy	866	0.01	0.03
Krishna	16,900	1.92	3.42
Lena	0	0	1.07
Mackenzie	0	0	5.43
Magdalena	1980	0.07	1.97
Mahakam	64,800	7.06	6.29
Mahanadi	101,900	1.73	3.51
Mekong	1,910,000	6.51	5.82
Mississippi	480,000	18.5	19.9
Moulouya	7470	6.49	6.46
Niger	59,000	0.69	3.26
Nile	1,300,000	1.53	2.08
Orinoco	34,200	21.3	21.0
Parana	267	0.04	0.53
Po	312	0.65	0.80
Rhine	43,900	2.04	4.00
Rhone	2590	2.63	5.56
Rio Grande	3930	0.13	1.69
Sao Francisco	5720	9.04	11.23
Sebou	7180	4.36	3.30
Senegal	23,800	3.95	1.59
Shatt el Arab	54,300	4.45	3.34
Tana	392	7.25	5.68
Volta	6320	1.13	1.12
Yangtze	484,000	1.07	3.17
Yellow	3760	0.57	1.02
Yukon	31	2.06	1.98
Zhuijiang	25,500	0.20	0.39
World	8,710,000	2.0	4.9

5.5. ESLR and storm surges

In many deltas, particularly in tropical and sub-tropical regions, storm surges are of particular concern and can raise sea level dramatically in a short period of time. Long term ESLR will result in a greater area inundated by storm surges (Church and Gregory, 2001). The Bengal delta has seen devastating storms with storm surges of up to 6 m (Haq, 1997), including events in 1970 and 1991 that resulted in approximately 500,000 and 150,000 deaths, respectively (Ali, 1996). Similarly,

Table 7
Estimated delta population at risk under baseline conditions extended from 2000 through 2050. The percentage of population at risk and area potentially lost relate to the total population and area of deltas covered in this study for each continent

	2050				
	Total delta population at risk	% continental delta population at risk	Avg % delta population at risk	% continental delta area potentially lost	Avg % delta area potentially lost
Asia	6,570,000	2.0	2.6	3.7	3.8
North America	512,000	6.8	5.0	9.7	5.8
South America	111,000	1.5	2.3	5.5	3.4
Europe	51,700	2.1	2.6	4.0	4.0
Africa	1,400,000	1.5	3.6	2.5	3.4
Oceania	64,000	6.9	3.7	5.5	3.8
Total	8,710,000	2.0	3.7	4.9	4.9

the Yangtze delta is vulnerable to typhoons, and resulting storm surges as high as 5.2 m have been measured (Chen, 1997). Historic storm surge values for the Bengal and Yangtze deltas were used to estimate the potential population and delta area impacted under potential storm conditions. When extended through 2050, the baseline ESLR in the Bengal Delta increases the delta population exposed to storm surge conditions from 44.9% to 47.3% and the delta area flooded from 47.0% to 49.8%. In the Yangtze delta the baseline ESLR under such storm conditions increases the delta population influenced from 28.3% to 30.1% and the delta area inundated from 42.6% to 43.9%. While the increase in the percent of population impacted is relatively small for each delta, it represents an additional 4.7 million and 0.84 million people living under conditions of vulnerability in the Bengal and Yangtze deltas, respectively.

6. Summary and conclusions

Using a newly developed data set of delta attributes, we applied a method to estimate the ESLR in individual deltas based on fluvial sediment inputs to the deltas, natural rates of delta subsidence, accelerated subsidence resulting from groundwater and hydrocarbon withdrawal, and rates of eustatic sea-level rise. The method was applied to a sample of 40 deltas distributed across a wide range of climatic, geomorphological, and economic development conditions. The contributing drainage basins associated with the 40 sampled deltas represent 30% of the global landmass and 42% of the water discharged by rivers entering the coastal zone. A combination of published measurements and straightforward assumptions is used to model natural subsidence within these deltas. Sediment loss by upstream trapping in reservoirs and flow diversion is accommodated in the estimate of fluvial sediment accretion on the deltas. In the absence of adequate measurements for the majority of deltas in the study, a method was established to estimate accelerated subsidence arising from local irrigation groundwater and hydrocarbon withdrawals and assumptions about the relationship between the natural subsidence and this accelerated subsidence.

Under baseline conditions, estimates of ESLR rates for the sample of 40 deltas range from 0.5 to 12.5 mm yr^{-1}. We estimate that if the rate of ESLR should persist at current levels and no mitigative responses undertaken, 4.9% of the deltaic areas considered by this study and 8.7 million people could potentially be affected by coastal inundation by 2050.

The sources of this vulnerability are derived predominantly from human activities on the continental landmass. Our results suggest that decreased fluvial accretion resulting from sediment loss in upstream reservoirs and flow diversion is the primary factor defining ESLR in nearly 70% of the 40 deltas. Sediment trapping by reservoirs has been identified as a significant impediment to sediment delivery to the coastal zone (Vörösmarty et al., 2003; Syvitski et al., 2005); a recent study of sediment flux data for 145 rivers indicates that of the approximately 50% showing statistically significant trends, the majority have decreasing sediment loads (Walling and Fang, 2003). Loss of fluvial sediment input has already resulted in observed land loss and coastal erosion in many deltas, and these impacts will continue to occur as the demand for water resources increases. Of the approximately 1000 large dams (>15 m height) under construction in 2000, 78% are located in Asia, 12% in Europe (predominately Eastern) and 5% in Africa (IWPDC, 2000), where there are high population densities and increased potential vulnerability. The concentration of planned reservoirs indicates that in some areas, particularly Asia, fluvial sediment trapping will continue to be an issue for the foreseeable future.

The direct impacts of ESLR in deltas include inundation of coastal areas, saltwater intrusion into coastal aquifers, increased rates of coastal erosion and an increased exposure to storm surges. These threats have implications to human populations in deltaic areas as well as in ecologically sensitive and important coastal wetland and mangrove forests. A recent study estimated that eustatic sea-level rise alone could result in the loss of 22% of the world's coastal wetlands by 2080 and that when combined with human impacts on wetlands, losses could reach 70% (Nicholls et al., 1999). The serious nature of the potential impacts of ESLR both on humans and the coastal resource base upon which we depend for a variety of services argues for improved and expanded studies in this realm. The recent emphasis on climate-related sea-level rise, which we find to be a relatively minor influence on the overall condition of deltaic systems, suggests that we are today poorly prepared to respond to the broad array of other critical determinants of coastal system stability well into the future. Deltas are particularly vulnerable to the combined effects of landward and seaward-derived forces and future studies must combine terrestrial and coastal ocean perspectives. Recent advances in remote sensing and increased availability of high resolution, large-scale data sets of elevation, population, land cover, and associated bio-geophysical factors have the potential to provide improved surveillance of ESLR and ESLR-associated impacts on the world's deltas. Greater awareness of potential threats to such systems is a precursor to the design of responses that maximize the protection of life, infrastructure and economic development.

References

Alam, M., 1996. Subsidence of the Ganges–Brahamaputra Delta of Bangladesh and associated drainage, sedimentation and salinity problems. In: Milliman, J.D., Haq, B.U. (Eds.), Sea-Level Rise and Coastal Subsidence. Kluwer Academic Publishers, pp. 169–187.

Ali, A., 1996. Vulnerability of Bangladesh to climate change and sea-level rise through tropical cyclones and storm surges. Water, Air, and Soil Pollution 92, 171–179.

Arnaud-Fassetta, G., 2003. River channel changes in the Rhone Delta (France) since the end of the Little Ice Age: geomorphological adjustment to hydroclimatic change and natural resource management. Catena 51, 141–172.

Bansil, P.C., 2004. Water Management in India. Concept Publishing Company, New Delhi, India.

Barusseau, J.P., Ba, M., Descamps, C., Diop, E.S., Diouf, B., Kane, A., Saos, J.L., Soumare, A., 1998. Morphological and sedimentological changes in the Senegal River after the construction of the Diama dam. Journal of African Earth Sciences 26, 317–326.

Bobba, A.G., 2002. Numerical modeling of salt-water intrusion due to human activities and sea-level change in the Godavari Delta, India. Hydrological Sciences Journal 47, S67–S80.

Bondesan, M., Minarelli, A., Russo, P., 1986. Studio dei movimenti verticali del suolo nella provincial di Ferrara. Proceeding Convegno Nazionale di Studi Storici, Comacchio, pp. 17–28.

Carson, M.A., Conly, F.M., Jasper, J.N., 1999. Riverine sediment balance of the Mackenzie delta, Northwest Territories, Canada. Hydrological Processes 13, 2499–2518.

Cencini, C., 1998. Physical processes and human activities in the evolution of the Po Delta, Italy. Journal of Coastal Research 14, 774–793.

Chen, J., 1997. The impact of sea-level rise on China's coastal areas and its disaster hazard evaluation. Journal of Coastal Research 13, 925–930.

Church, J., Gregory, J.M., 2001. Changes in sea-level. In: Houghton, J. T., Ding, Y., Griggs, D.J., Noguer, M., van der Linden, P.J., Dai, X., Maskell, K., Johnson, C.A. (Eds.), Climate Change 2001: the Scientific Basis. Contribution of Working Group 1 to the Third Assessment Report of the Intergovernmental Panel on Climate Change. Cambridge University Press, Cambridge.

Coleman, J.M., 1976. Deltas: Processes of Deposition and Models for Exploration. Continuing Education Publication Company, Inc., Champaign, IL.

Coleman, J.M., Wright, L.D., 1971. Analysis of Major River Systems and their Deltas: Procedures and Rationale, with Two Examples. Coastal Studies Series Number 28Louisiana State University, Baton Rouge, La.

Collins, M., Evans, G., 1986. The influence of fluvial sediment supply on coastal erosion in West and Central Africa. Journal of Shoreline Management 2, 5–12.

Day, J.W., Pont, D., Hensel, P.F., Ibanez, C., 1995. Impacts of sea-level rise on deltas in the Gulf of Mexico and the Mediterranean: the importance of pulsing events to sustainability. Estuaries 18, 636–647.

Day, J.W., Britsch, L.D., Hawes, S.R., Shaffer, G.P., 2000. Pattern and processes of land loss in the Mississippi delta: a spatial and temporal analysis of wetland habitat change. Estuaries 23, 425–438.

Douglas, B.C., 2001. Sea-level change in the era of the recording tide gauge. In: Douglas, B.C., Kearney, M.S., Leatherman, S.P. (Eds.), Sea-Level Rise: History and Consequence. Academic Press, San Diego, pp. 37–61.

Douglas, B.C., Peltier, W.R., 2002. The puzzle of global sea-level rise. Physics Today 55, 35–41.

Dynesius, M., Nilsson, C., 1994. Fragmentation and flow regulation of river systems in the northern third world. Science 266, 753–762.

Fanos, A.M., 1995. The impact of human activities on the erosion and accretion of the Nile Delta coast. Journal of Coastal Research 11, 821–833.

FAO, 1974. Soil Map of the World. Food and Agriculture Organization of the United Nations—United Nations Educational, Scientific and Cultural Organizations, Paris.

FAO, 2004. AQUASTAT Agricultural Water Use Statistics. Food and Agricultural Organization of the United Nations, Paris, France.

Federer, C.A., Vörösmarty, C.J., Fekete, B., 2003. Sensitivity of annual evaporation to soil and root properties in two models of contrasting complexity. Journal of Hydrometeorology 4, 1276–1290.

Fekete, B.M., Vörösmarty, C.J., Lammers, R.B., 2001. Scaling gridded river networks for macroscale hydrology: development, analysis, and control of error. Water Resources Research 37 (7), 1955–1967.

Fetter, C.W., 2001. Applied Hydrogeology, 4th edition. Prentice Hall, Inc.

Gastaldo, R.A., Allen, G.P., Huc, A.Y., 1995. The tidal character of fluvial sediments of the modern Mahakam River delta Kalimantan, Indonesia. In: Flemming, B.W., Bartholomae, A. (Eds.), Tidal Signatures of Modern and Ancient Sediments. Special Publication of the International Association of Sedimentologists, vol. 24, pp. 171–181.

GESAMP, 1994. Anthropogenic Influences on Sediment Discharge to the Coastal Zone and Environmental Consequences. GESAMP Reports and Studies No. 52GESAMP (Joint Group of Experts on the Scientific Aspects of Marine Environmental Protection).

Giosan, L., Bokuniewicz, H., Panin, N., Postolache, I., 1999. Longshore sediment transport pattern along the Romanian Danube Delta Coast. Journal of Coastal Research 15, 859–871.

Green, P.A., Vorosmarty, C.V., Meybeck, M., Galloway, J.N., Peterson, B.J., Boyer, E.W., 2004. Pre-industrial and contemporary fluxes of nitrogen through rivers: a global assessment based on typology. Biogeochemistry 1, 1–35.

Haq, B.U., 1997. Regional and global oceanographic, climatic and geological factors in coastal zone planning. In: Haq, B.U., Haq, S. M., Kullenber, G., Stel, J.H. (Eds.), Coastal Zone Management Imperative for Maritime Developing Nations. Kluwer Academic Publishers, pp. 55–74.

Ibe, A.C., 1996. The Niger Delta and sea-level rise. In: Milliman, J.D., Haq, B.U. (Eds.), Sea-Level Rise and Coastal Subsidence. Kluwer Academic Publishers, pp. 249–267.

ICOLD, 1998. World Register of Dams. International Commission on Large Dams, Paris, France.

Inman, D.L., Nordstrom, C.E., 1971. On the tectonic and morphologic classification of coasts. The Journal of Geology 79, 1–21.

IWPDC, 2000. International Water Power and Dam Construction Yearbook 2000. Wilmington Publishing Ltd.

Jelgersma, S., 1996. Land subsidence in coastal lowlands. In: Milliman, J.D., Haq, B.U. (Eds.), Sea-Level Rise and Coastal Subsidence. Kluwer Academic Publishers, pp. 47–62.

Jiongxin, X., 2003. Growth of the Yellow River Delta over the past 800 years, as influenced by human activities. Geografiska Annaler 85, 21–30.

Kesel, R.H., 1988. The decline of the suspended load of the lower Mississippi river and its influence on adjacent wetlands. Environmental Geological Water Sciences 11, 271–281.

Kesel, R.H., 1989. The role of the Mississippi River in wetland loss in southeastern Louisiana, USA. Environmental Geological Water Sciences 13, 183–193.

Kolb, C.R., Dornbusch, W.K., 1975. The Mississippi and Mekong deltas—a comparison. In: Broussard, M.L. (Ed.), Deltas: Models for Explorations. Houston Geological Society, pp. 193–207.

Leatherman, S.P., Zhang, K., Douglas, B.C., 2000. Sea-level rise shown to drive coastal erosion. EOS 81, 55–57.

L'Homer, A., 1992. Sea-level changes and impacts on the Rhone coastal lowlands. In: Tooley, A., Jelgersma, S. (Eds.), Impacts of Sea-Level Rise on European Coastal Lowlands. Blackwell Publishers, Oxford.

Ly, C.K., 1980. The role of the Akosombo Dam on the Volta River in causing coastal erosion in central and eastern Ghana (West Africa). Marine Geology 37, 323–332.

Maldonado, A., 1975. Sedimentation, stratigraphy, and development of the Ebro Delta, Spain. In: Broussard, M.L. (Ed.), Deltas: Models for Explorations. Houston Geological Society, pp. 311–317.

McManus, J., 2002. Deltaic responses to changes in river regimes. Marine Chemistry 79, 155–170.

Meybeck, M., Ragu, A., 1996. GEMS/water contribution to the global register of river inputs. GEMS/Water Programme (UNEP/WHO/UNESCO). World Health Organization, Geneva, Switzerland.

Meybeck, M., Vörösmarty, C.J., 2005. Fluvial filtering of land to ocean fluxes: from natural Holocene variations to Anthropocene. Comptes Rendus 337, 107–123.

Miller, L., Douglas, B.C., 2004. Mass and volume contributions to twentieth-century global sea-level rise. Nature 428, 406–409.

Milliman, J.D., 1997. Effect of terrestrial processes and human activities on river discharge, and their impact on the coastal zone. In: Haq, B.U., Haq, S.M., Kullenberg, G., Stel, J.H. (Eds.), Coastal Zone Management Imperative for Maritime Developing Nations. Kluwer Academic Publishers, pp. 75–92.

Milliman, J.D., Broadus, J.M., Gable, F., 1989. Environmental and economic implications of rising sea-level and subsiding deltas: the Nile and Bengal examples. Ambio 18, 340–345.

Mohanti, M., 1993. Coastal processes and management of the Manadi River deltaic complex, east coast of India. In: Kay, R. (Ed.), Deltas of the World. American Society of Civil Engineers, pp. 122–137.

Nicholls, R.J., 2002. Rising sea-levels: potential impacts and responses. In: Hester, R.E., Harrison, R.M. (Eds.), Issues in Environmental Science and Technology: Global Environmental Change, vol. 17, pp. 83–107.

Nicholls, R.J., Hoozemans, F.M.J., Marchard, M., 1999. Increasing flood risk and wetland losses due to global sea-level rise: regional and global analysis. Global Environmental Change 9, s69–s87 (Special Issue).

Nilsson, C., Reidy, C.A., Dynesius, Revenga, C., 2005. Fragmentation and flow regulation of the world's large river systems. Science 308, 405–408.

Onu, N.C.H., 2003. The oil rich Niger Delta region: a framework for improved performance of the Nigerian regulatory process. Ambio 32, 325–326.

ORNL (Oak Ridge National Laboratory), 2002. Landscan population dataset. Available at: http://www.ornl.gov/sci/gist/landscan/2002.

Panin, N., Jipa, D., 2002. Danube River sediment input and its interaction with the north-western Black Sea. Estuarine, Coastal and Shelf Science 54, 551–562.

Penland, S., Ramsey, K.E., 1990. Relative sea-level rise in Louisiana and the Gulf of Mexico: 1908–1988. Journal of Coastal Research 6, 323–342.

Pont, D., Day, J.W., Hensel, P., Franquet, E., Torre, F., Rioual, P., Ibanez, C., Coulet, E., 2002. Response scenarios for the deltaic plain of the Rhone in the face of an accelerated rate of sea-level rise with special attention to Salicornia-type environments. Estuaries 25, 337–358.

Poulos, S.E., Collins, M.B., 2002. Fluviate sediment fluxes to the Mediterranean Sea: a quantitative approach and the influence of dams. In: Jones, S.J., Frostick, L.E. (Eds.), Sediment Flux to Basins: Causes, Controls and Consequences. Special Publications, vol. 191. Geological Society, London, pp. 227–245.

PRB, 2004. Population Reference Bureau: Population and Health Data. www.prb.org2004.

Pruszak, Z., Symytkiewicz, M., Hung, M.N., Ninh, P.V., 2002. Coastal processes in the Red River Delta area, Vietnam. Coastal Engineering Journal 44, 97–126.

Rachold, V., Grigoriev, M.N., 2000. Russian–German Cooperation System Laptev Sea 2000: The expedition LENA 99. Reports on Polar Research 354.

Raghavendra Rao, V., 1991. Giant Petroleum Accumulations in Delta Environments. Memoirs—Geological Society of India, vol. 20, pp. 95–108.

Rainwater, E.H., 1975. Petroleum in deltaic sediments. In: Broussard, M.L. (Ed.), Deltas: Models for Explorations. Houston Geological Society, pp. 3–11.

Ramkumar, M., 2003. Progradation of the Godavari Delta — a fact or empirical artifice? Insights from coastal landforms. Journal of the Geological Society of India 62, 290–304.

Rao, K.N., Sadakata, N., 1993. Holocene evolution of deltas on the east coast of India. In: Kay, R. (Ed.), Deltas of the World. American Society of Civil Engineers, pp. 1–5.

Reed, D.J., 2002. Sea-level rise and coastal marsh sustainability: geological and ecological factors in the Mississippi delta plain. Geomorphology 48, 233–243.

Ren, M., 1993. Relative sea-level rise in Huanghe, Changjiang and Zhuijiang (Yellow, Yangtze and Pearl River) deltas over that last 30 years and prediction for the next 40 years (2030). Acta Geographica Sinica/Dili Xuebao 48, 385.

Ren, M., Milliman, J.D., 1996. Effect of sea-level rise and human activity on the Yangtze Delta, China. In: Milliman, J.D., Haq, B.U. (Eds.), Sea-Level Rise and Coastal Subsidence. Kluwer Academic Publishers, pp. 205–214.

Rodolfo, K.S., 1975. The Irrawaddy Delta: tertiary setting and modern offshore sedimentation. In: Broussard, M.L. (Ed.), Deltas: Models for Explorations. Houston Geological Society, p. 344.

Sanchez-Arcilla, A., Jimenez, J.A., Valdemoro, H.I., 1998. The Ebro Delta: morphodynamics and vulnerability. Journal of Coastal Research 14, 754–772.

Sestini, G., 1992. Implications of climatic changes for the Po delta and Venice lagoon. In: Jeftic, L., Milliman, J.D., Sestini, G. (Eds.), Climatic Change and the Mediterranean. Edward Arnold, London.

Sestini, G., 1996. Land subsidence and sea-level rise: the case of the Po Delta region, Italy. In: Milliman, J.D., Haq, B.U. (Eds.), Sea-Level Rise and Coastal Subsidence. Kluwer Academic Publishers, pp. 235–248.

Shuttleworth, W.J., Wallace, J.S., 1985. Evaporation from sparse crops: an energy combination theory. Quarterly Journal of the Royal Meteorological Society 111, 839–855.

Siebert S., Döll, P., Hoogeven, J. 2002 Global map of irrigated areas version 2.1 Center for Environmental Systems Research, University of Kassel, Germany, Food and Agriculture Organization of the United Nations, Rome, Italy.

Snoussi, M., Haida, S., 2002. Coastal changes in response to the effects of dam construction on the Moulouya and the Sebou River (Morocco). In: Arthurton, R.S., Kremer, H.H., Odada, E., Salomans, W., Marshall, J. (Eds.), African Basins: LOICZ Global Change Assessment and Synthesis of River Catchment–Coastal Sea Interaction and Human Dimensions. Texel, pp. 123–129.

Stanley, J.D., 1990. Recent subsidence and northeast tilting of the Nile Delta: rapid rates, possible causes, and consequences. Marine Geology 94, 147–154.

Stanley, J.D., 1996. Nile Delta: extreme case of sediment entrapment on a delta plain and consequent coastal land loss. Marine Geology 129, 189–195.

Stanley, J.D., Randazzo, G., 2001. Petrologic database to define the human reworked, sediment-deficient plain of the Rio Grande Delta, Texas. Environmental Geology 41, 37–53.

Stanley, J.D., Warne, A.G., 1994. Worldwide initiation of Holocene marine deltas by deceleration of sea-level rise. Science 265, 228–231.

Stanley, J.D., Warne, A.G., 1998. Nile Delta in its destructive phase. Journal of Coastal Research 14, 794–825.

Stevenson, J.C., Ward, L.G., Kearney, M.S., 1986. Vertical accretion rates in marshes with varying rates of sea level rise. In: Wolfe, D.A. (Ed.), Estuarine Variability. Academic Press, New York, pp. 241–259.

Syvitski, J.P.M., Vörösmarty, C.V., Kettner, A.J., Green, P., 2005. Impact of humans on the flux of terrestrial sediment to the global coastal ocean. Science 308, 376–380.

USGS, 2003. GTOPO30 Elevation Dataset. United States Geological Survey EROS Data Center, Sioux City, United States.

Vörösmarty, C.V., Sharma, K.P., Fekete, B.M., Copeland, A.H., Holden, J., Marble, J., Lough, J.A., 1997. The storage and aging of continental runoff in large reservoir systems of the world. Ambio 26, 210–219.

Vörösmarty, C.V., Federer, C.A., Schloss, A.L., 1998. Potential evaporation functions compared on US watersheds: possible implications for global-scale water balance and terrestrial ecosystem modeling. Journal of Hydrology 207, 147–169.

Vörösmarty, C.V., Fekete, B., Meybeck, M., Lammers, R.B., 2000. A simulated topological network representing the global system of rivers at 30-minute spatial resolution (STN-30). Journal of Hydrology 237, 17–39.

Vörösmarty, C.V., Meybeck, M., Fekete, B., Sharma, K., Green, P., Syvitski, J., 2003. Anthropogenic sediment retention: major global impact from registered river impoundments. Global and Planetary Change 39, 169–190.

Vörösmarty, C.J., Douglas, E.M., Green, P.A., Revenga, C., 2005. Geospatial indicators of emerging water stress: an application to Africa. Ambio 34, 230–236.

Walling, D.E., Fang, D., 2003. Recent trends in the suspended sediment loads of the World's Rivers. Global and Planetary Change 39, 111–126.

Waltham, T., 2002. Sinking cities. Geology Today 18, 95–100.

Wang, J., 1998. Sea-level changes, human impacts and coastal responses in China. Journal of Coastal Research 14, 31–36.

Wells, J.T., 1996. Subsidence, sea-level rise, and wetland loss in the Lower Mississippi River Delta. In: Milliman, J.D., Haq, B.U. (Eds.), Sea-Level Rise and Coastal Subsidence. Kluwer Academic Publishers, pp. 281–311.

Wells, J.T., Coleman, J.M., 1984. Deltaic morphology and sedimentology, with special reference to the Indus River Delta. In: Haq, B. U., Milliman, J.D. (Eds.), Marine Geology and Oceanography of Arabian Sea and Coastal Pakistan. Van Nostrand Reinhold Co., New York, pp. 85–100.

Wilmott, C.J., Feddema, J.J., 1992. A more rational climatic moisture index. Professional Geographer 44, 84–87.

Wright, L.D., Coleman, J.M., Erickson, M.W., 1974. Analysis of Major River Systems and their Deltas: Morphologic and Process Comparisons. Technical Report, vol. 156. Coastal Studies Institute, Louisiana State University, Baton Rouge.

Yang, Z., Milliman, J.D., Galler, J., Liu, J.P., Sun, X.G., 1998. Yellow River's water and sediment discharge decreasing steadily. EOS 79, 589–592.

Yang, Z., Saito, Y., Lui, B., Zhang, J., Wang, H., 2002. Decadal and Millennial Time-Scale Changes of Water and Sediment Discharge of the Huanghe (Yellow River) caused by Human Activities. LOICZ Reports and Studies, vol. 26. LOICZ.

Yu, Liansheng, 2002. The Huanghe (Yellow) River: a review of its development, characteristics, and future management issues. Continental Shelf Research 22, 389–403.